44TH TURBOMACHINERY & 31ST PUMP SYMPOSIA
HOUSTON, TEXAS | SEPETEMBER 14 – 17 2015
GEORGE R. BROWN CONVENTION CENTER

The Measured Impact of Erosion on the Rotodynamic and Performance Characteristics of a Mixed Flow ESP

Gerald L. Morrison
Professor of Mechanical Engineering
Texas A&M University
College Station, Texas USA

Nicolas Carvajal
Graduate Student
Texas A&M University
College Station, Texas USA

Ramy Saleh
Graduate Student
Texas A&M University
College Station, Texas USA

Changrui Bai
Graduate Student
Texas A&M University
College Station, Texas USA

ABSTRACT

Three stages of a mixed flow electric submersible pump were subjected to 117 hours of erosion using a 2 gram/liter concentration ratio of 100 mesh hydraulic fracture sand to water. The sand passed through the pump one time and is discarded. The wear of flow paths and bearings is presented along with variation in pump performance and vibration as the pump wears. The pump was operated at its Best Efficiency Point (BEP) which is 1150 GPM (30100 BPD) at 3600 RPM with a specific speed of 1600. The hydraulic performance of the pump decreased 6.3% due to wear occurring in the secondary flow paths. Specifically, the bearings and seals were severely worn with bearing orbits up to 50 mils peak to peak. At the end, the bearings had worn more than the seals resulting in the seals carrying the rotordynamic loads of the rotor. Microscopic investigation of the tungsten carbide sleeve bearings showed what are believed to be thermal stress cracks which were revealed after the surface of the bearings were eroded.

INTRODUCTION

The natural flow of mature oil or gas fields drops below economic production rates after a period of production. When reservoir pressure drops, the need for artificial lifting systems become crucial to support the required operating flow rates. The Electrical Submersible Pump was introduced to the petroleum industry by the pump inventor Armais Artunoff in 1927. Since then, ESP systems continued to grow, especially and historically in high water cut oil wells. According to Schlumberger's Oilfield review of summer 2004 [1], the Electrical Submersible Pump (ESP) system is the second most applied artificial lift system globally after the Sucker Rod. In 2004, there was an estimated number of 100,000 operating ESP systems in producing wells worldwide and this number continues to grow. ESPs are known for their high volume flow rates and have been widely used by the oil and gas industry for artificial lift. As on shore oil reservoir resources face depletion, oil and gas explorations turn to offshore, subsea and ultra-deep subsea reservoirs to continue extracting the precious minerals and naturally ESPs followed. Today's challenges and requirements of ESP systems continue to push ESP research to have longer life spans, handle multiphase flows, resist abrasive erosion and maximize operating efficiency.

There are two types of impellers used in ESPs: radial flow and mixed flow impellers. Radial flow impellers are typically used for lighter applications where the flow is less than 3,000 BPD and mixed flow impellers are used on larger capacity pumps (up to 40,000 BPD). The current pump under investigation has mixed flow impellers.

The inherent problem created by the placement of ESPs in subsea wells, besides the impracticality and difficulty of periodic maintenance, is the high cost of installation and removal of the pump. The cost of removing and installing a faulty pump could be, depending on the depth, up to forty times the cost of a new pump. For this reason, more emphasis is now being placed on research to extend the useful life of the pump to at least five years, and to locate, predict and mitigate any and all causes of pump failure.

One possible cause of submersible pump failure, depending on the nature of the oil bearing strata, is the damage incurred to the bearings, shaft and other components due to the presence of fine sand in the fluid. The sand present in the fluid originates either from the well itself or from the hydraulic fracturing of the well and thus its type, size and concentration will vary from well to well. Most wells have some type of sand control, usually gravel pack covered with a mesh. This will filter out the coarser gravel, but finer sands will seep through the mesh. The fine sand can pass through the product-lubricated bearings and small clearances inside the pump, creating erosion problems, which in turn can lead to wear, vibration and possible pump failure.

A custom-made for laboratory environment, fixed impeller mixed flow electrical submersible pump is used for this study (referred from now on as ESP). For space constraint issues and unavailability of a well in the laboratory, only three stages of the pump were tested and, since standard ESP motors

are designed to be inserted inside the well, a regular 250 HP induction motor is used instead. The three stages of the pump are installed inside a special casing built for the sole purpose of the laboratory experiment. The pump was operated at its initial BEP during the erosion study.

Framo Engineering tested centrifugal pumps passing 300 tons of sand through pumps at concentrations of 0.02, 0.2 and 2 grams of sand per liter of water. The results showed that the higher concentration is required to obtain significant erosion in a reasonable time period. This is the basis for the 2 grams/liter concentration used for this study.

The pump under consideration has a specific speed of 1600 for the operating conditions used. A typical cross section of a mixed flow pump with flow from the bottom to top is show at the right. The pump studied has an impeller diameter of 10.25 inches. When subjected to fluids extracted directly from a well there may be solid particles present in the flow. Since most wells undergo hydraulic fracturing, some of these solids may be the sand used which typically runs from 70 to 100 mesh. The purpose of this study was to determine how the presence of 100 mesh hydraulic fracturing sand affects the pump over a period of time.

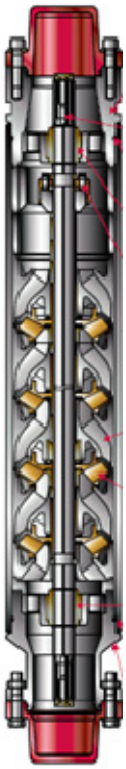

Figure 1. Typical ESP Pump Section

EXPERIMENTAL FACILITIES

A facility to perform erosion studies was designed and constructed for this project. Figure 2 shows a schematic of the facility. Sand is loaded into a hopper from which a variable speed auger is used to convey sand into a stand pipe feeding a small centrifugal pump. This pump provides about 5% of the water required by the ESP but has all of the sand passing through it. This is done so that the Coriolis flow meter can accurately measure the amount of sand and water passing through the pump. This information is used to adjust the speed of the auger to maintain an overall ESP sand load of 5 grams/liter. The other 95% of the water passes through a separate pump and the flow rate is metered using an orifice flow meter. The water source is from the clean water side of a hydro cyclone separator system which removes the sand as it exits the ESP.

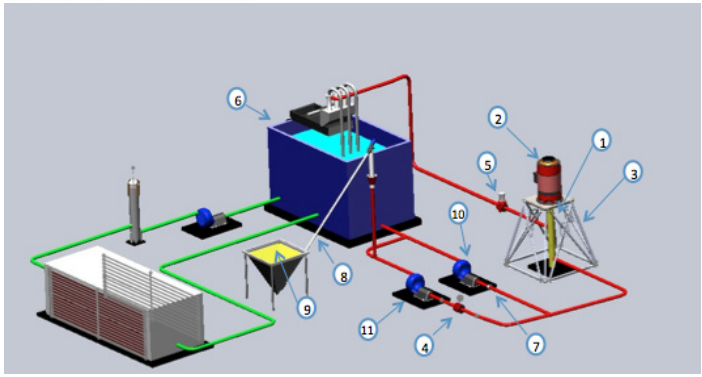

Figure 2. Experimental Setup Diagram. The red piping represents the test loop, green piping represents the cooling loop.

No.	Item
1	ESP Pump
2	ESP Motor
3	Derrick
4	Coriolis Flow Meter
5	Pinch Valve
6	Tanks and Separators
7	Orifice Flow Meter
8	Sand Auger
9	Sand hopper
10	Feed Pump
11	Slurry Pump

Table 1 Identification for items in Figure 2.

The two supply pumps' flows are combined and provide an inlet pressure of 40 psig to the ESP which exceeds the minimum required to prevent cavitation in the ESP. The flow passes through the ESP, through a choke, and into the separator system. Here, the sand is removed and discarded. The sand passes through the pump only one time allowing a constant input parameter.

Table 2 provides a sieve analysis of the sand used in the study. Figure 3 presents a microscope photograph of a sand sample taken at the Turbomachinery Laboratory.

Sieve Analysis of Submitted Proppant Samples
From Sierra Frac Sand, LLC
ISO 13503-2/API RP19C, Section 6, "Sieve Analysis"

Sample I.D.	Sample: 100 Mesh Sierra Gold	
US Standard Sieve No.	Weight % Retained	Cumulative
6	0.0	0.0
8	0.0	0.0
10	0.0	0.0
12	0.0	0.0
14	0.0	0.0
16	0.0	0.0
18	0.0	0.0
20	0.0	0.0
25	0.0	0.0
30	0.0	0.0
35	0.0	0.0
40	0.2	0.2
45	0.8	1.0
50	0.9	1.8
60	9.1	10.9
70	23.8	34.7
80	26.5	61.2
100	18.0	79.2
120	12.8	91.9
140	5.5	97.4
170	2.0	99.5
200	0.4	99.9
230	0.0	99.9
pan	0.1	100.0
total	100.0	
in-size	95.6	= as 50/140
ISO Mean Dia. (mm)	0.195	
Median Dia. (mm)	0.187	

Table 2. Sand Sieve Analysis Results

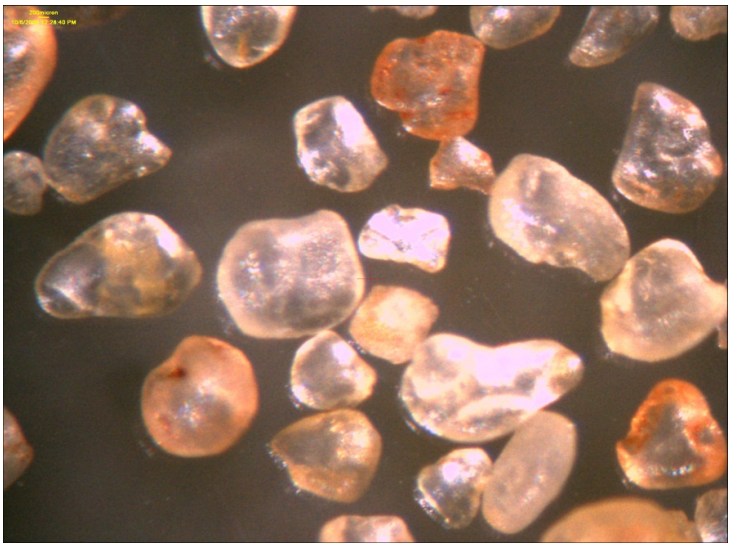

Figure 3. Microscope photograph of sand.

The pressure into and out of the pump was continuously monitored along with power to the pump, flow rate through the pump, and the output from two 3D accelerometers mounted on the top and bottom flanges of the pump. In addition, proximeter probes were inserted into the pump at set time intervals to measure the actual vibration motion of the rotor. The proximeter and accelerometer data were recorded using a simultaneous A/D system.

RESULTS

Pump Performance

The three performance parameters that were monitored through the 117 hours of erosion testing are efficiency, power, and total head. The general performance is shown in Figure 4. The figure compares the pump performance after 117 hours of erosion in plotted dots to the baseline data shown in solid lines. The mean efficiency dropped 6.8% and the pump's mean total head dropped 6.3% after 117 hours of erosion testing. However, the mean power consumption did not show much change with a 0.5% increase. This indicates that the impellers are still supplying a relatively constant amount of energy to the fluid flow. For this pump, the seals wore significantly while the main hydraulic paths showed only minor erosion. It is therefore concluded that the decrease in head was due to increased leakage from each stage's exit to its inlet by way of the secondary flow paths. Details of the hydraulic paths wear are included later in this paper.

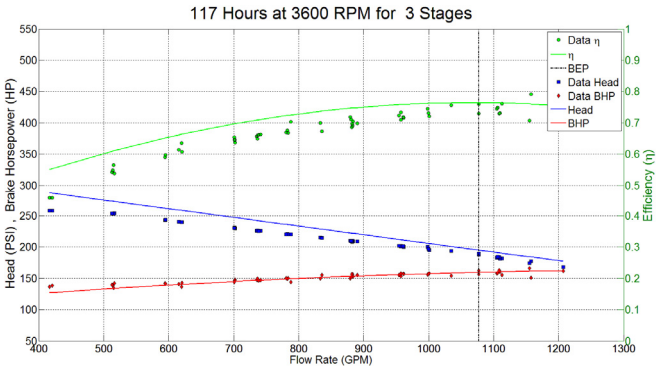

Figure 4. Pump performance change due to 117 hours of erosion.

Impellers

The ESP pump in this study contains three impellers made of cast iron with a Nedox coating that has a yellowish color on the entire surface. This coating gives the impeller properties such as high abrasion resistance, corrosion resistance, increased surface hardness, and reduced coefficient of friction. The impeller is a double shrouded, mixed flow type, fixed, 10.25" impeller. It has five vanes and five axial balancing holes as seen in Figures 5 and 6. The balancing holes are important to reduce the thrust force on the impeller but they do result in hydraulic losses. Each impeller was balance checked for rotational balance by the manufacturer.

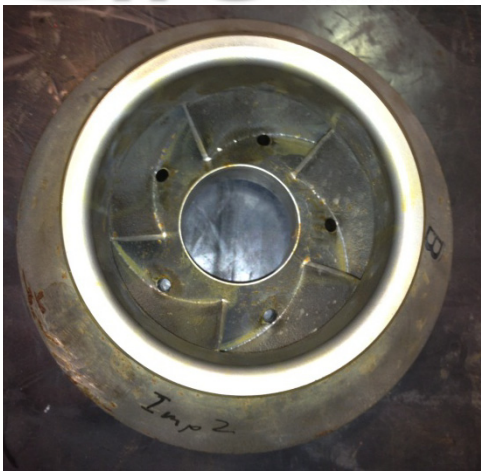

Figure 5. Second stage impeller intake

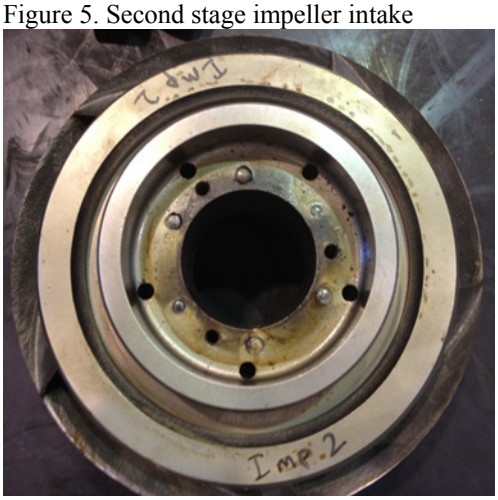

Figure 6. Second stage impeller discharge

Each impeller has two labyrinth seals on its top and bottom as seen in Figure 7. Each seal consists of four grooves with the function of restricting the fluid secondary flow paths. They are also an important component of pump rotor dynamics because they function as non-contact, centrifugal stabilizers during impeller rotation. Thus they help maintain shaft life, bearing life and pump life. Impeller dimensions including the labyrinth seal dimensions were measured periodically and weighed to monitor wear. Proximeter probes are also placed on the impeller seal to monitor shaft orbit and vibration. Pump performance curves are recorded periodically as well to monitor performance and compared to erosion and vibration data.

Figure 7. Second stage impeller side view

Diffusers

Another main component of the ESP is the diffuser or the volute casing. Diffusers function to convert dynamic pressure to static pressure as the fluid velocity decreases and the cross sectional area increases. There are three diffusers in the test pump each made out of cast iron and have no visible coatings. It is important to note that the vanes surfaces are left rough by the manufacturer. Each diffuser has seven vanes as shown in Figure 8. It is a mixed flow type diffuser that is set in an identical position relative to other diffusers along the pump to prevent clocking during assembly. Visible on the diffuser intake are two tubes passing through the flow path. These tubes are used to house the proximeter probes when they are installed so that the orbit of the shaft next to the bearing located in the diffuser can be measured. The diffuser housings for the labyrinth seals are smooth cylindrical surfaces.

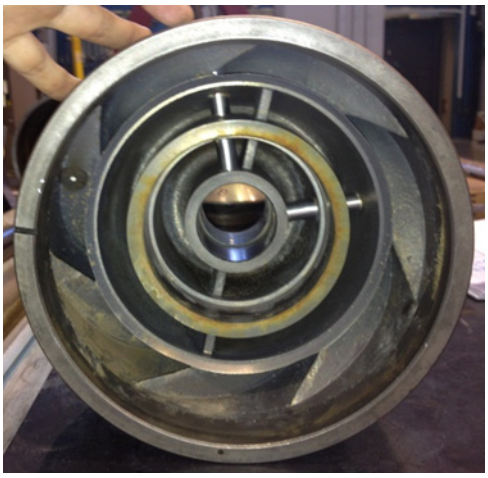

Figure 8. Stage one diffuser intake (top) and discharge.

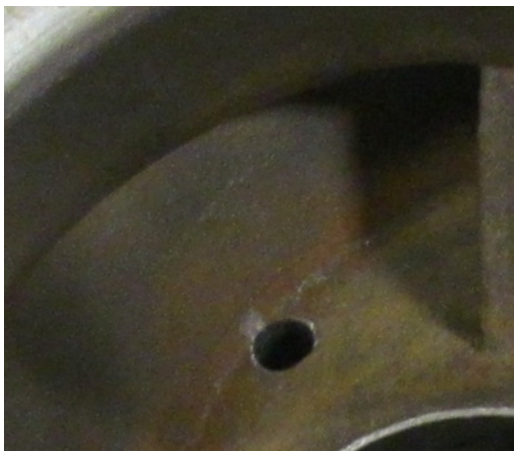

Figure 9. Impeller Balance Holes Base Condition, Inlet

The original impeller balance hole conditions are shown in Figure 9. Figure 10 illustrates that a groove due to erosion after 117 hours occurred on the main hydraulic flow side of the impeller. This groove is caused by the wake that is present behind the jet of fluid passing from the high pressure region behind the impeller into the main flow, much like erosion around bridge piers. The size of the groove changes from one stage to the other. Stage one has the smallest groove at the balance hole. Stage number two has a larger groove caused by erosion and stage number three has the largest groove due to erosion.

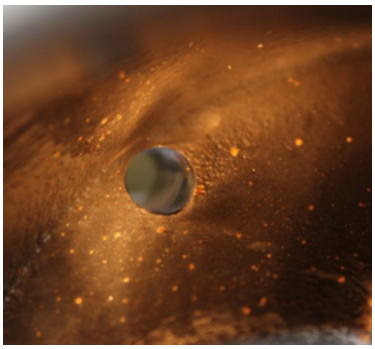

a) Stage 1

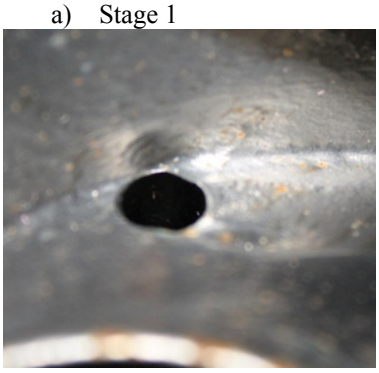

b) Stage 2

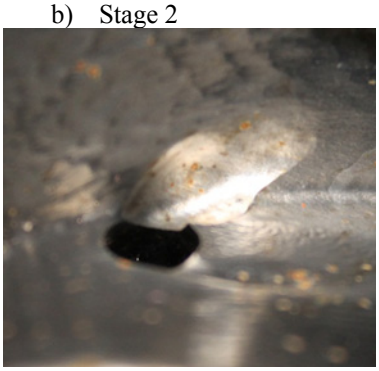

c) Stage 3

Figure 10. Impeller Balance Holes Intake Side after 117 Hours

The impeller erosion is visible on the impeller blades and walls. After 117 hours the blade tips are not straight (curved) and the blade edges became slimmer and sharper (Figure 11). The impeller walls are shiny due to the impinging effect of erosion. The walls also have signs of wear caused by the sand and eddy currents in the main flow paths.

a) 0 Hours

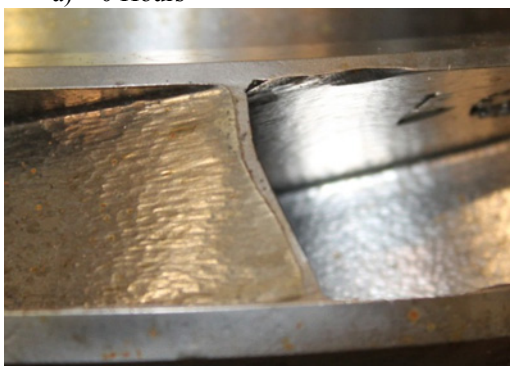

b) 117 Hours

Figure 11. Impeller Blades Base Condition before and after 117 Hours of Erosion

The diffusers primary flow path ways were painted at the start of the test to help visualize the areas affected by erosion. Figure 12 shows the initial condition on the top. Erosion affected the diffusers blade tips causing the ends to be round and smooth. The amount of erosion on the pressure side of the blades was more than the suction side. The diffuser walls lost all paint. The walls became smoother with signs of wear caused by the abrasive and the eddy currents produced in the main flow paths. The diffuser hub lost paint at areas that are on the pressure side of the diffuser blades.

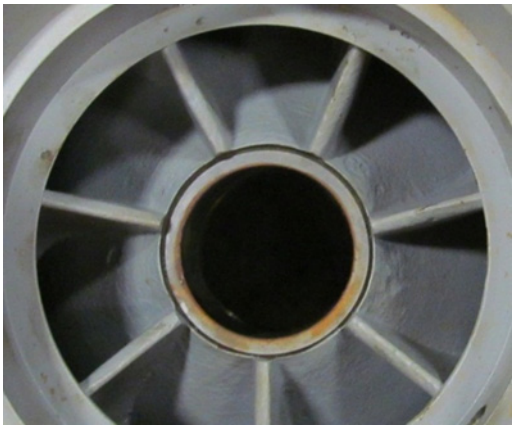

Figure 12. Diffuser Discharge at Base Condition (top) and After 117 Hours

After 117 hours the intake of the diffuser is presented in Figure 13. The diffuser walls are smoother with impinging erosion marks. The leading edge of the diffuser blades are curved with more signs of wear near the wall and hub. Wear at the intake of the diffuser is more visible than at the discharge.

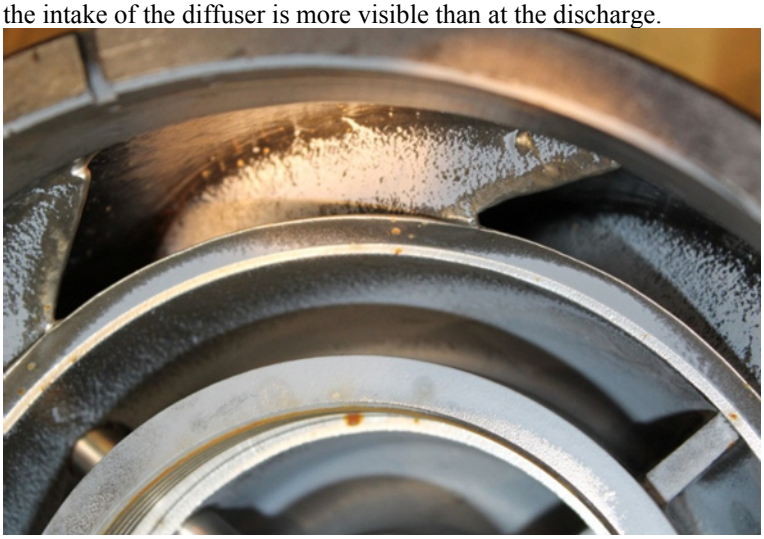

Figure 13. Diffuser Intake after 117 Hours

Seals

The impeller was originally coated with the yellow coating shown in Figure 14. This is an abrasion resistant coating placed on the impeller seals by the pump manufacturer to mitigate the rate of wear. After 24 hours this coating on all stages was completely eroded. The impeller seals wear due to erosion causes the seal clearances to increase and the seal groves to be shallower as later discussed in this section.

a) 8 Hours

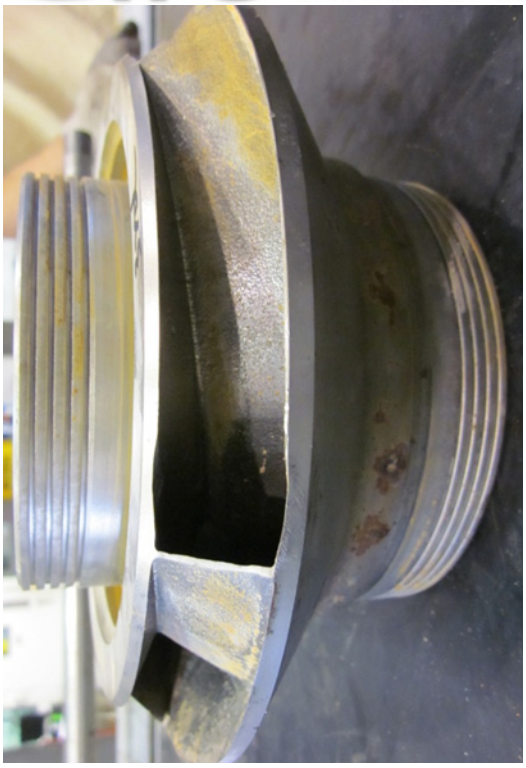

b) 24 Hours

c) 56 Hours

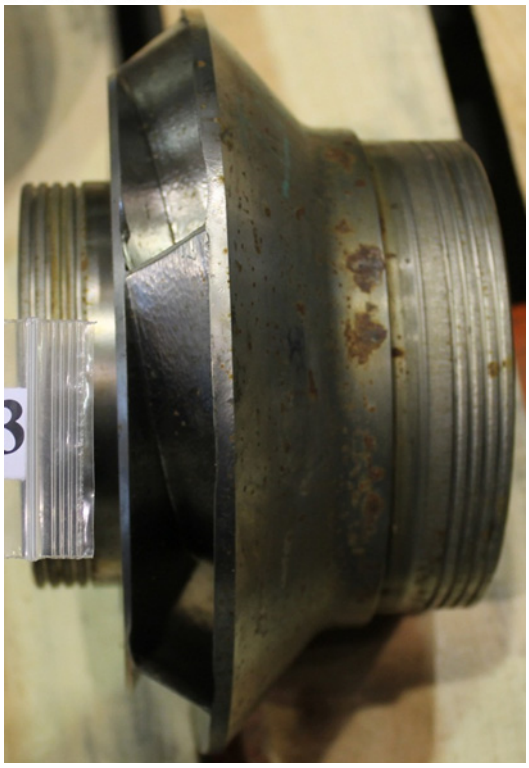

d) 117 Hours

Figure 14. Impeller three Condition after 8, 24, 56 and 117 Hours

The impellers discharge and diffusers intake labyrinth seal erosion is documented by the amount of material removed by erosion. These results are shown in Figure 15 where the values represent the decrease in impeller seal diameter and increase in the diffusers seal diameter. The combined value is the increase in diametrical clearance of the seal. The diffusers change in dimensions are negligible when compared to the impellers. Location affected the impellers rate of wear. The amount of wear in impeller 1 (pump inlet) is slightly less than the wear in impellers 2 and 3.

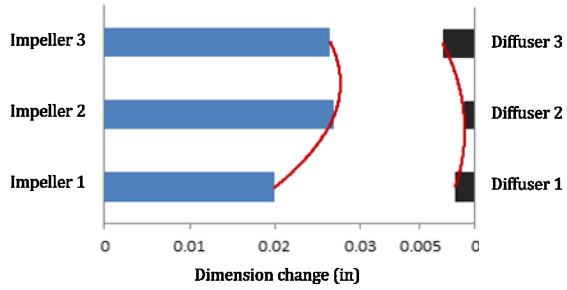

Figure 15. Impeller Discharge and Diffuser Intake Change in Dimension after 117 Hours

The impellers intake and diffusers discharge labyrinth seal changes in diameter are shown in Figure 16. The location of the impeller directly impacted their rate of wear as seen in Figure 16 where impeller 1 had the highest amount of wear followed

by impellers 2 and 3. Diffusers 1, which is coupled to impeller 2, had the same amount of dimension change as impeller 2. Diffuser 2, which is coupled to impeller 3, also had the same amount of dimension change as impeller 3. The diffusers rate of wear is also affected by location where diffuser 1 had more wear than diffuser 2. The 3rd diffuser is not coupled to an impeller. It had a negligible amount of change after 117 hours of erosion.

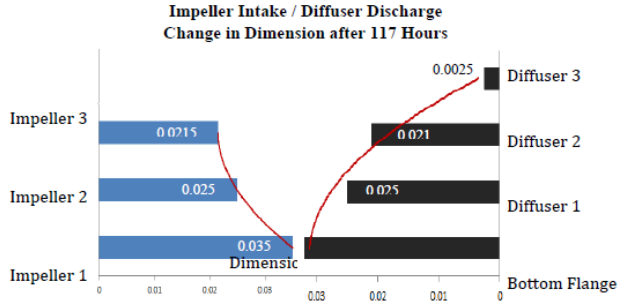

Figure 16. Impellers and Diffusers Wear Modes by Location (2)

Figures 17 and 18 further illustrate the sand erosion results by showing the labyrinth seal dimension and location at 0, 8, 24, and 117 hours of erosion. These evolution charts corresponds to the results previously discussed in the wear mode diagrams. It is important to distinguish between the two seals on the impellers and track their wear separately. The first type of labyrinth seal is located on the impellers discharge side and is coupled with the diffusers intake side as seen in Figure 17. The second type of labyrinth seal is located on the impellers intake side and is coupled with the diffusers discharge side as seen in Figure 18.

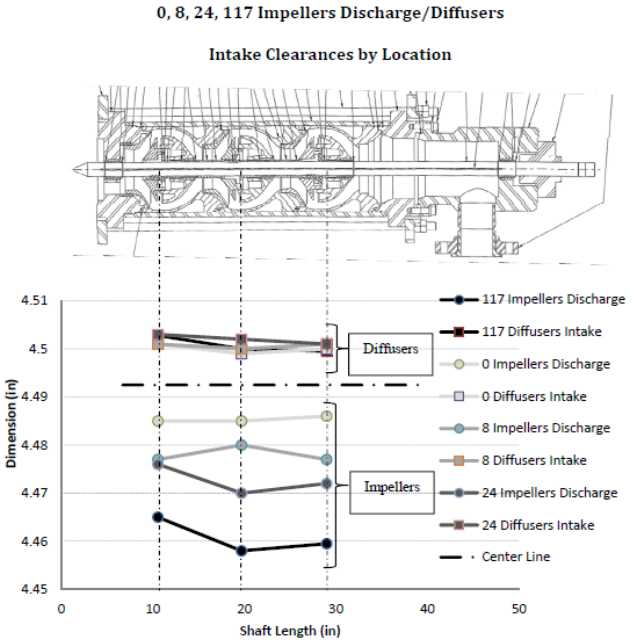

Figure 17. Impellers and Diffusers Evolution by Location (1)

Figure 17 shows a negligible amount of dimension change in the diffusers in all stages after 117 hours of erosion. The impellers dimensions significantly changed with time. The rate of wear is more on impellers 2 and 3 than on impeller 1.

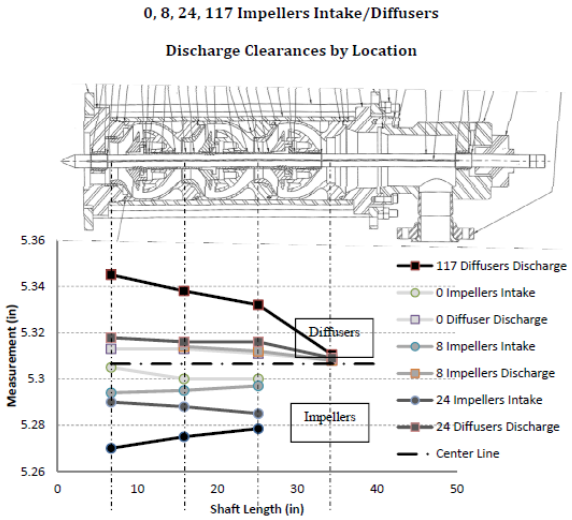

Figure 18. Impellers and Diffusers Evolution by Location (2)

Figure 18 shows the even wear measured in the impellers and diffusers. The 3rd diffuser's discharge is not coupled with an impeller and showed no wear. Impeller 1 intake is coupled with the brass bottom flange seal and had more wear than impellers 2 and 3. The rate of wear increases as the location moves away from the motor coupling towards the pump inlet.

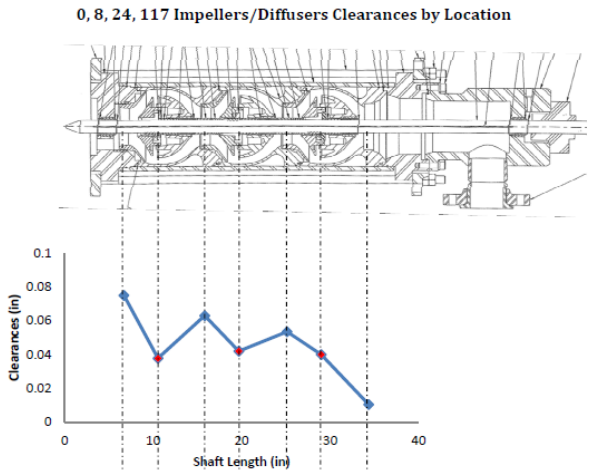

Figure 19. Impellers and Diffusers Clearances after 117 Hours by Location

Figure 19 presents the diametrical clearance of the seals after 117 hours of wear. The diffuser inlet seal has greater wear than the outlet seal.

The pump was disassembled at 56 and 117 hours of erosion. Figure 20 shows how the bearings eroded during the

study. Included are the OD and ID of the journal and bush as well as the net clearance. The cutaway of the pump shows the locations. The bearing wear decreases from the pump inlet (bottom of the pump) to the pump exit. The pump shaft is 1.5 inches in diameter. At the pump inlet, the maximum diametrical clearance was 0.050 inches resulting in a clearance to radius ratio of 0.033. The bearings were relatively ineffective at this point.

Bearings

The bearings used in this pump are constant diameter and clearance sleeve bearing. Both the journal and bush (sleeve and housing) are made of tungsten carbide.

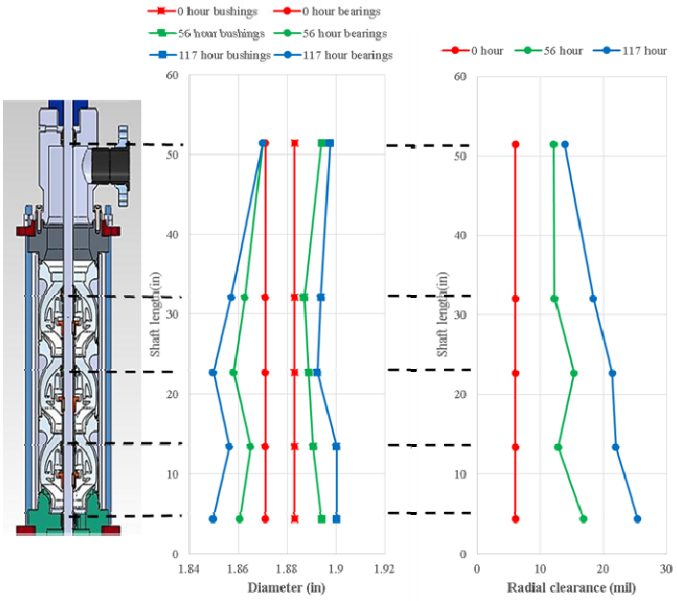

Figure 20. Bearing clearance changes due to erosion

Another interesting effect of the erosion is that the bearing (journal) diameter has more wear at the exit of each bearing than at the inlet as indicated by the smaller diameter, effectively generating a divergent taper. These data are shown in Figure 21. The arrows on the graphic indicate the direction of the leakage flow through the bearing. As the sand progresses through the bearing, it is initially crushed by the bearing as indicated by the circumferential grooves around the bearing. This produces smaller sand particles which have sharp fracture edges. These smaller particles work as an abrasive material to more rapidly erode the bearing and to provide a polished surface.

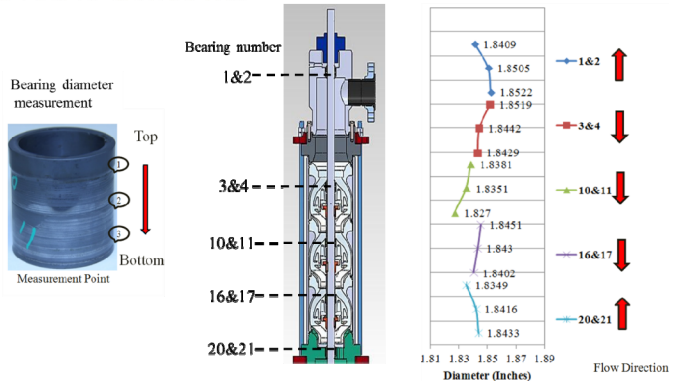

Figure 21. Bearing (journal) diameter variation along length. Red arrows show direction of flow.

Microscopic examination of the bearings is shown in Figures 22 and 23. These bearing assemblies had a radial clearance of 0.006 inch when new. The 100 mesh sand has an average size of 0.006 inch. Therefore the sand is able to enter into the bearing clearance. The four images are of two different bearing (journal) surfaces at different locations in the pump. For each location, one image is near the leakage flow's entrance and the second is near the exit. The two are different in that at the inlet the large grains of sand are crushed inside the bearing as the clearance varies in the azimuthal direction. The rotation of the shaft in the direction of decreasing clearance grabs the sand and drags it around the bearing. This is evidenced by the circular grooves in the bearing surface. By the time the sand exits the bearing clearance, the sand size has been reduced by the crushing affect producing smaller sand grains with sharp edges. The sand has the effect of a polishing compound. A very interesting result is that the outside surface of the bearing is cleanly removed revealing that the inner portion of the bearing has a well ordered array of stress cracks covering the entire surface. It is hypothesized that these cracks are caused by thermal stress occurring when the bearing surfaces rub, heating the surfaces causing them to expand. Due to the low thermal conductivity of the tungsten carbide, the inner regions remain cool and are fractured due to the expansion of the outer surface. Since this pump was operated with less than a 20F temperature variation, thermal shock due to fluid temperature variations were not possible. The depth of the fine cracks has not been established at this point but if they significantly penetrate the radius of the bearing, the structural integrity of the bearing will be greatly reduced. More study is required to evaluate this affect. The Turbomachinery Laboratory is constructing a bearing test facility to study this in detail.

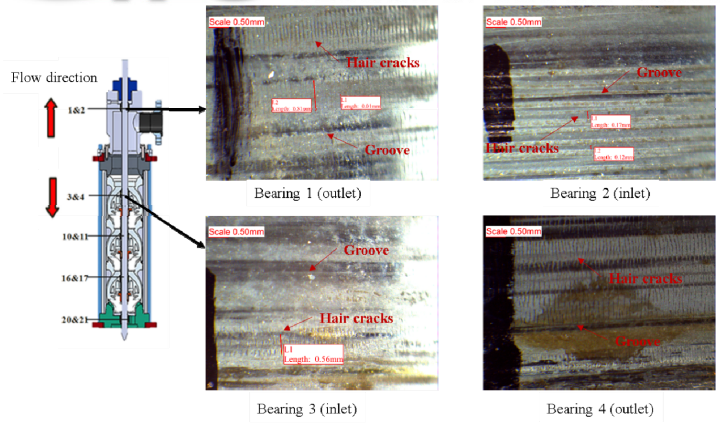

Figure 22. Microscopic examination of the bearing (journal) surface for the exit bearings at 117 hours.

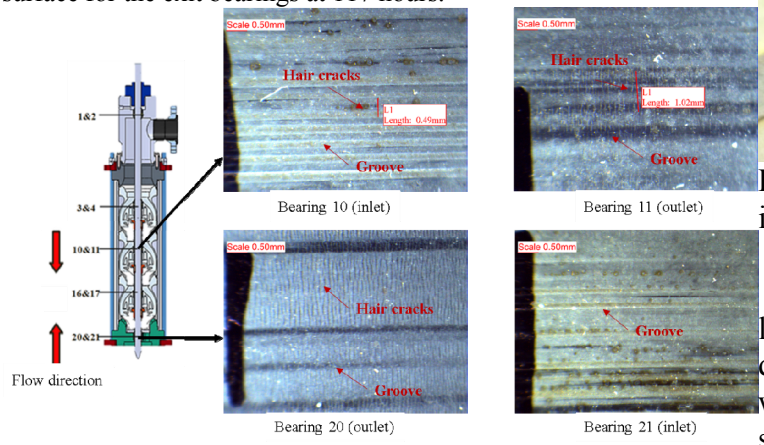

Figure 23. Microscopic examination of the bearing (journal) surface for the inlet and center bearings at 117 hours.

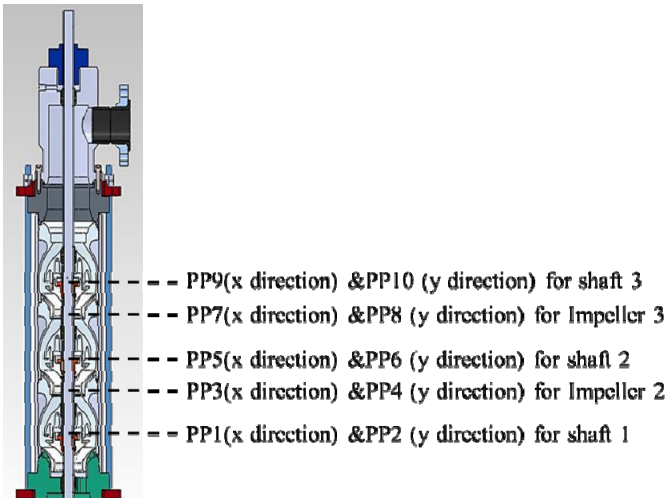

Figure 24. Proximeter probe locations.

Figure 25. Photograph of proximeter probes installed in pump.

Figure 26 presents orbits for the five axial locations instrumented recorded at different times during the erosion process. The first two impellers were monitored along with the three bearings that support the two impellers as shown in Figure 24. Impeller 2 has spikes on it since flat spots were machined onto it to facilitate rotor angle measurement. The shaft locations are for the shaft bearings' motion with the impeller being the orbit of the impeller located between the bearings in the position indicated in Figure 24.

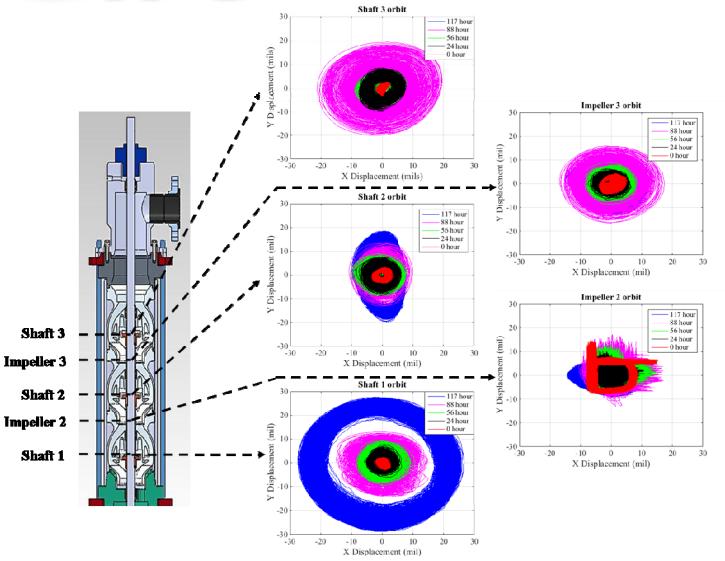

Figure 26. Pump components orbits at various stages of erosion.

As Figure 20 has indicated, the bearing at the pump inlet (Shaft 1) has the most wear and the orbits tend to be circular. Shaft 2 has a significantly smaller orbit which begins relatively circular but become elliptical at the end of the study. Shaft 3 bearing maintains a relatively circular orbit with a maximum amplitude between Shaft 1 and Shaft 2 bearings. The interesting observation is that the two impeller seals have ultimate orbits smaller than Shaft 1 and 3 while Shaft 2 is smaller. It appears that as the wear progresses the impeller seals are starting to replace the bearings as the load carrying component. Figure 27 combines the data of the physical diameters of the bearings and seals into one figure. It can be seen that as the erosion progresses the clearance of the bearings exceed the clearance of the impeller seals by a considerable amount. The impeller seals ultimately reach a radial clearance of 20 mils while the bearing range from 26 to 32 mils. This is further evidence that the impeller seals have become the pump bearings.

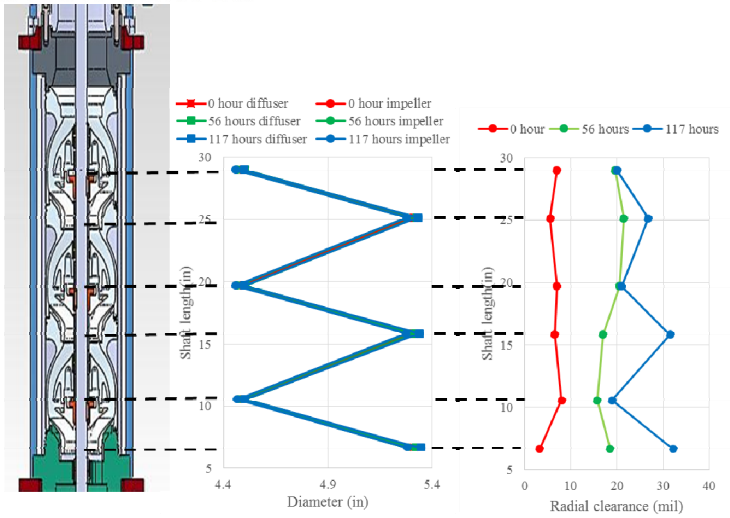

Figure 27. Radial clearances between impellers and diffusers at different erosion times.

The evolution of the frequency content of the pump vibrations due to erosion as indicated by the PP1 proximeter probe for the Shaft 1 location are shown in Figures 28 and 29. Water fall spectra of how the vibration of the pump changed with erosion time is presented in Figure 28 for one of the proximeter probes. At the start, the primary vibration is at the pump speed with a 2X harmonic and a slight indication of 1/3 and 2/3 components. As wear progressed, the sub harmonic components increased with the 2/3 component becoming dominant at the end of the test. Also included in Figure 29 is a ramp up water fall plot showing how the 2/3 harmonic tracks with the speed of the pump.

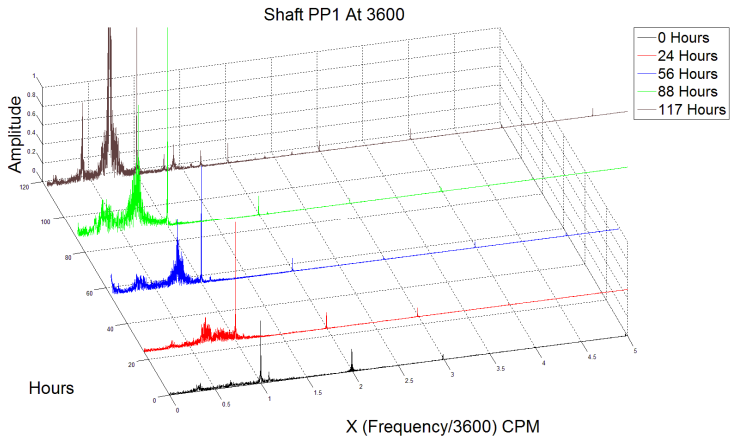

Figure 28. Shaft 1 (PP1) orbit frequency content variation with erosion.

Figure 28

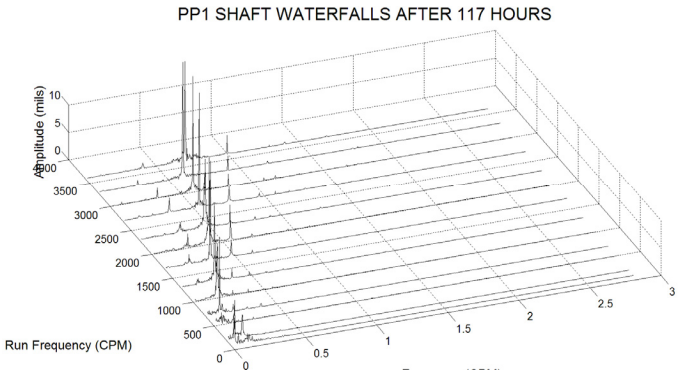

Figure 29. Shaft 1 (PP1) start up waterfall plot after 117 hours of erosion.

Since there are two primary frequencies present in the spectra which change in dominance with wear, the contribution of each to the orbit of the pump components was investigated. Figures 30 and 31 present the amplitude and phase (relative Shaft 3) of the 60 Hz (3600 RPM, run speed) and 40 Hz components. These data were obtained using spectral analysis of the proximeter probe data. All the data were obtained using a simultaneous A/D system so that phase information is maintained. A band of frequencies were used centered about the two specified frequencies. The fundamental (60 Hz) component has amplitudes below 5 mils for the entire erosion process. The phase varies about 90° initially but increases to over 180° after 117 hours indicating a change in the vibrational mode. The sub-synchronous mode has the largest amplitude reaching a maximum of 12 mils at 117 hours. The values at 0 hours are not shown since they are less than 1 mil. The phase change is essentially constant indicating a whirling type instability precessing at 2/3 the pump running speed.

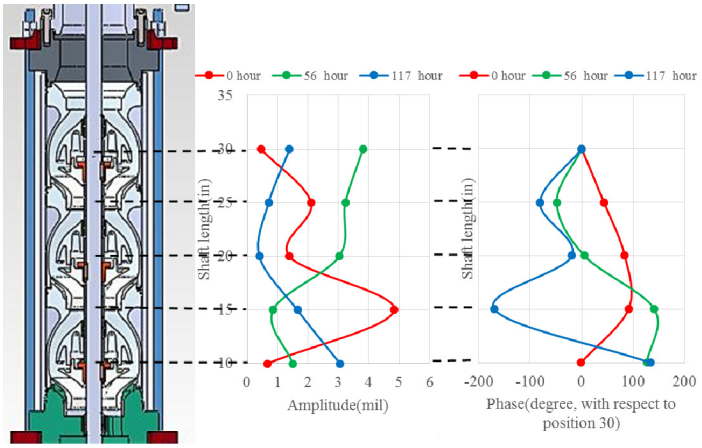

Figure 30. Synchronous vibration amplitude and phases (60Hz).

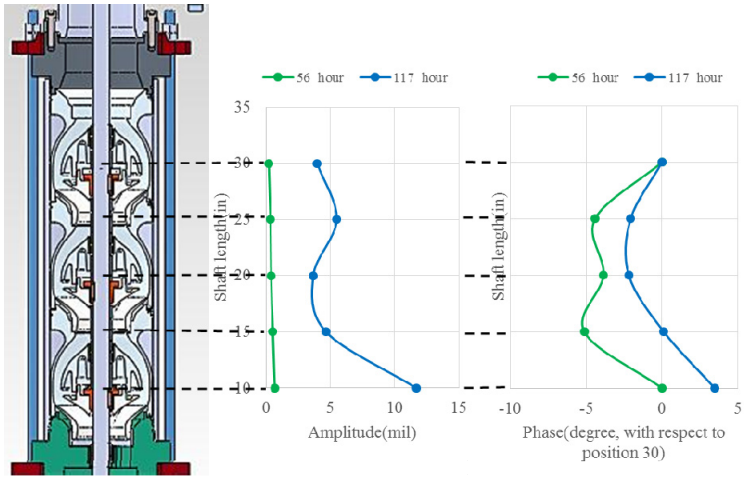

Figure 31. Sub-synchronous vibration amplitude and phases (40Hz).

Figures 32 to 34 present animations showing the orbit of the rotor as measured by the five sets of proximeter probes. The first, third and fifth points are the three bearings supporting the second and third impellers, points two and four. The top graph is for the entire unfiltered proximeter probe data. The middle graph presents the orbits for the 3600 RPM (60 Hz) component and the bottom figure is for the 2400 RPM (40 Hz) component. The filtered components were obtained using Fast Fourier Transform techniques to apply a bandpass filter of sufficient breadth around the desired frequency to capture the motion as indicated by the spectrum presented in Figure 28.

Figure 32 presents the initial startup condition (0 hours) of the pump. The 60 Hz component and the unfiltered data show the rotor vibration is contained primarily in the 60 Hz component. The 60 Hz component clearly shows a phase change along the axis of the pump. The 40 Hz component is presented on a scale the expands the motion by a factor of five and shows a constant phase indicating a whirling motion. The bearings have the smaller orbits than the impellers. The spikes on the oribit for impeller 2 are flats that were machined onto the seal for phase reference.

Figure 33 presents the results at 56 hours. All three graphs have the same scales on the motion. The amplitudes of the motion at the bearings are increasing more rapidly than the impellers. Again,

most of the motion is in the 60 Hz mode whose phase varies along the pump axis. The 40 Hz whirling mode is increasing in amplitude reaching a maximum at the pump inlet.

Figure 34 presents the results at 117 hours. The axis scales of the top and bottom graphs are three times larger than the center (60 Hz) scale. At this point the whirling (40 Hz) mode dominates the vibration of the pump. These data also clearly show that the orbits of the shaft at the bearings are considerably larger than the orbits of impellers 2 and 3. This indicates that the impellers have essentially become the bearings.

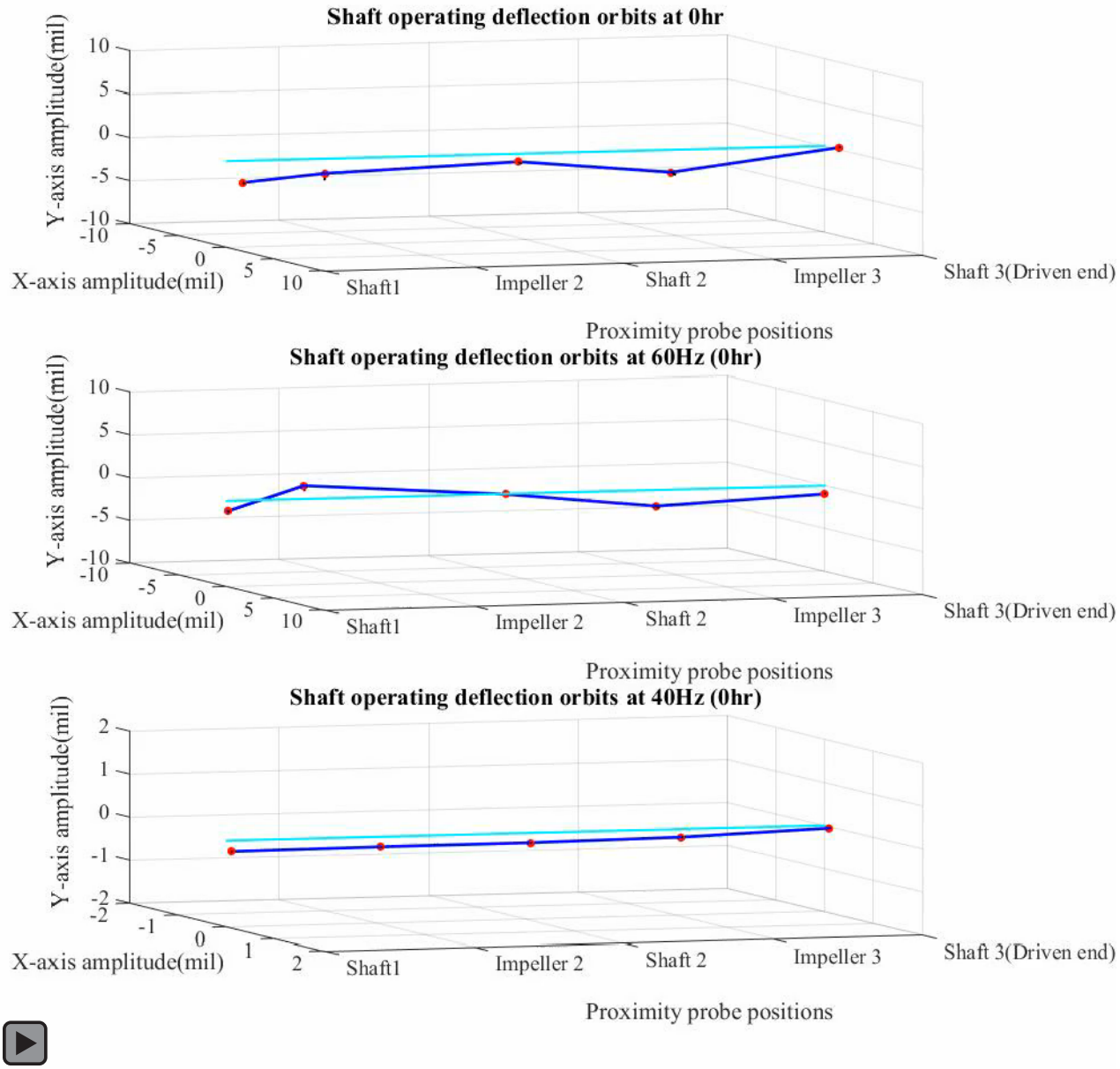

Figure 32. Rotor orbits at 0 hours.

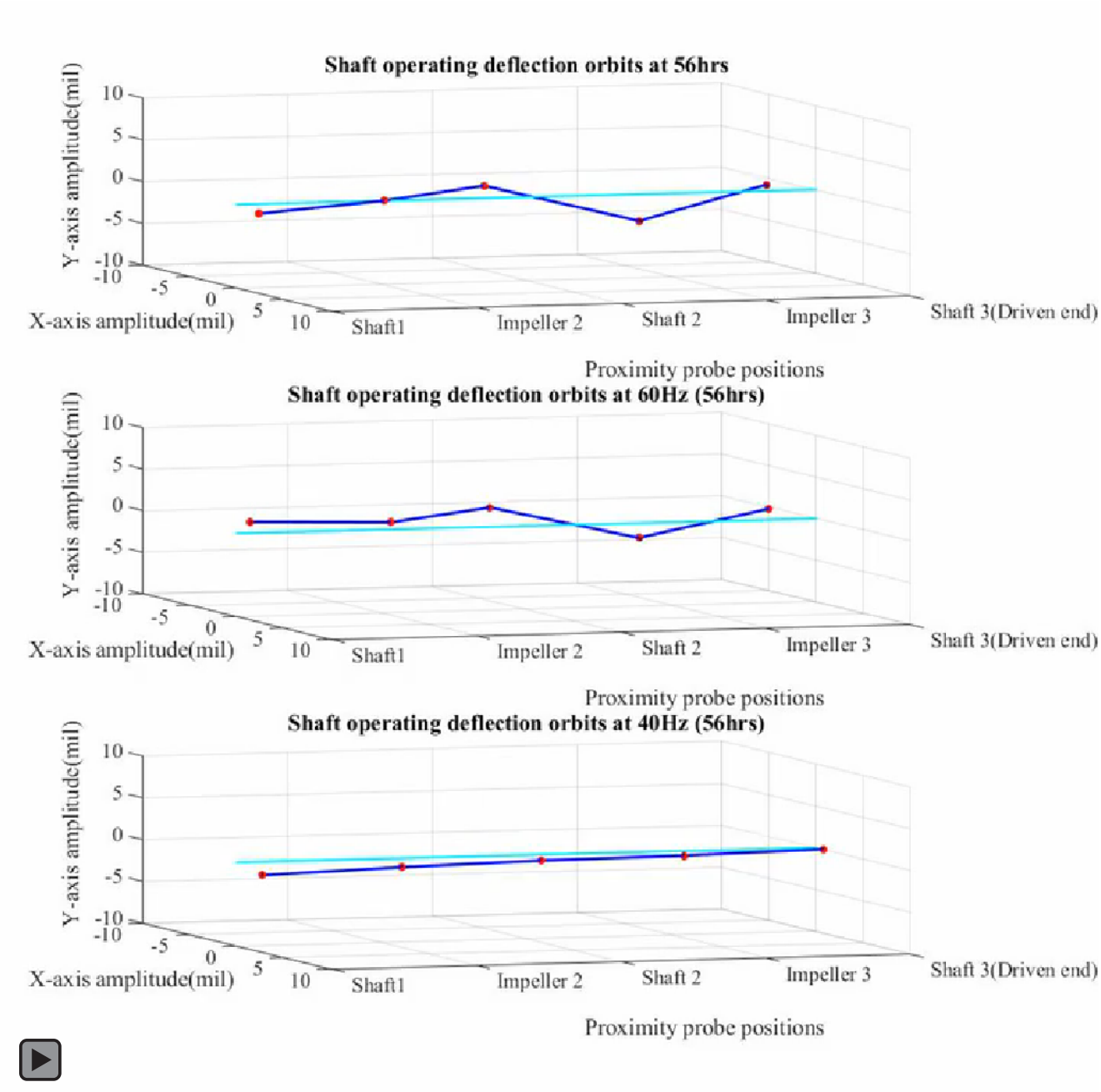

Figure 33. Rotor orbits at 56 hours.

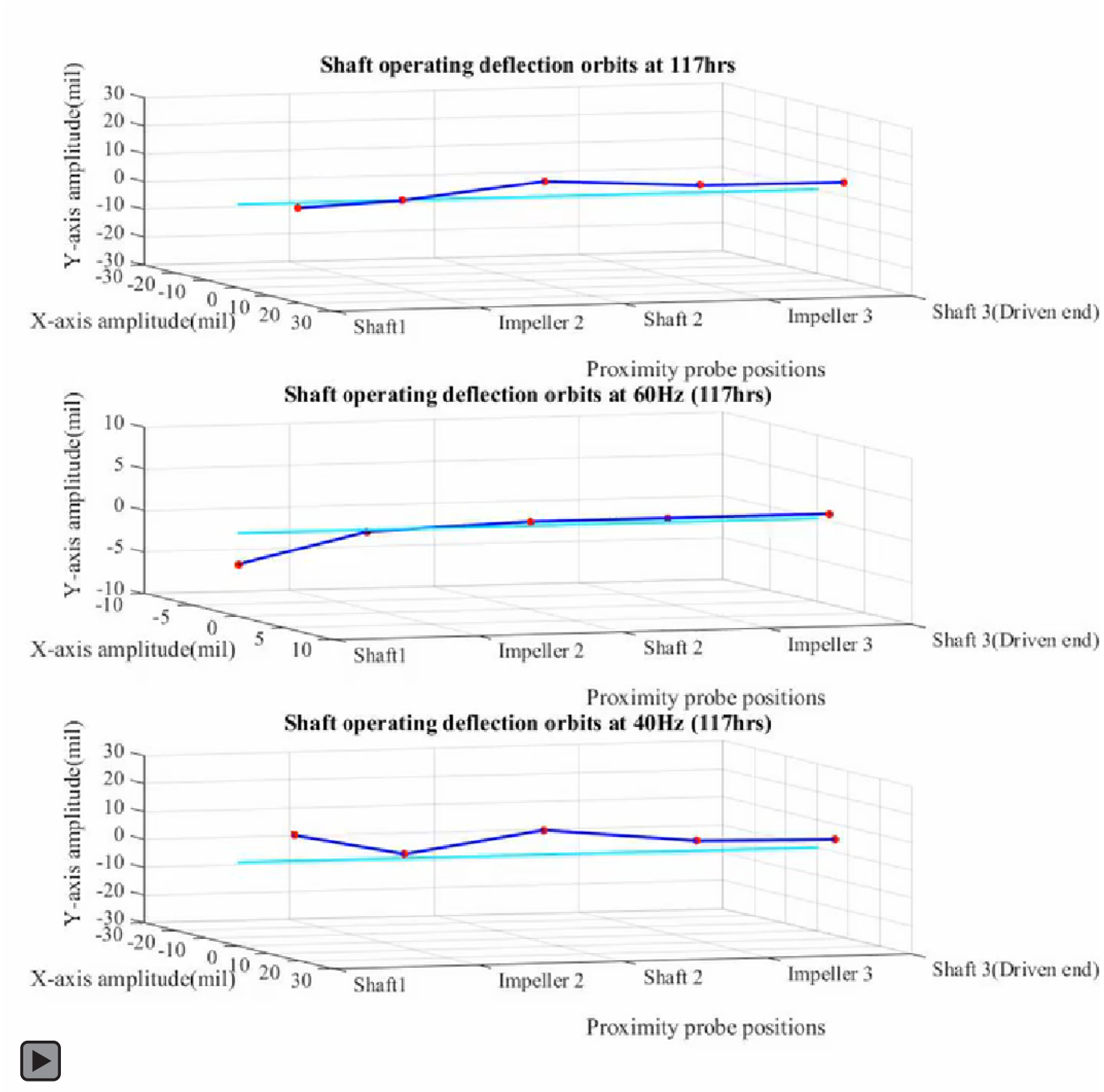

Figure 34. Rotor orbits at 117 hours.

CONCLUSIONS

The experimental testing of a mixed flow ESP undergoing sand slurry erosion using 100 mesh fracture sand at 2 grams per liter concentration operating at 3600 RPM, 1150 PSI pressure rise, 40 PSI inlet pressure, 1600 specific speed, and vertical operating position showed significant wear to the pump components after 117 hours. The study also showed a decrease in pump performance and an increase in vibration as a direct result to the wear taking place in the pump.

The wear patterns in the pump components due to abrasive erosion are divided into impingement wear and shear wear. Shear wear took place on the pump bearings, and corresponding bushings, impeller downstream seals, impeller upstream seals, and their corresponding diffuser stators, opening the clearances which reduced the stiffness of the entire system. This type of wear is caused by the friction of sand between a stator and a rotor, and it directly impacts the secondary flow paths of the pump. The amount of shear wear on the bearings and impeller downstream seals is higher at the pump intake and gradually decreases across the stages to the pump discharge. There are three reasons for this difference in wear rate between the stages. The first reason is that the sand at the pump intake is sharpest and most aggressive as it gets crushed in the first stage. As the sand moves from one stage to the other, the sand loses its sharpness causing lesser shear wear to the final stage components. The second reason is that the pump is vertically placed under the motor. The system is stiffer at the drive end of the pump which also happens to be the pump discharge. On the other hand, the pump intake is 52 inches away from the drive end of the shaft so it is hanging free and has less stiffness. This variation in stiffness directly resulted in smaller amount of wear and clearances near the drive end and larger amounts of wear away from the drive end. The third reason for this difference in rate of wear due to location is the pressure difference across the stages. At the pump intake, more sand gets trapped between stators and rotors due to the low pressure difference across the first stage. The entrapment of sand allows more wear to occur in the components affected. As the pressure differences increase from one stage to the other, less sand is trapped in the discharge stage between stators and rotors so less wear takes place at the pump's third stage.

The second type of wear is caused by impinging sand particles that affect the diffusers and impellers hub, walls, and blades that shape the primary flow paths of the pump. Impingement wear can also be seen on the impellers balance holes, thrust plate and the spacers that are in the pump's secondary flow paths. The amount of balance hole wear after 117 hours is small at the first stage impeller and grows larger at the second stage impeller and grows much larger at the third stage impeller. It is important to note that the sand size is constant through the test and that as clearances grow sand erosion effect is reduced. This is because the sand particles become small enough to flow through the larger seal clearances. The variation in the amount of wear from one stage to the other is caused by the difference in pressure rise across the stages as previously discussed. The higher the pressure rise the more backflow takes place through the secondary flow paths.

The wear measured or captured after 117 hours of erosion testing had a direct impact on the pump's performance. The pump's overall efficiency dropped 6.8%, the total delivered pressure rise across three stages fell 6.3%, the best efficiency point dropped 0.8% and the electric power consumption increased 0.5%. These results indicate that the pump is consuming more power to deliver lesser pressure rise and efficiency than the base condition. The primary cause to the drop in pressure rise is the recirculation of the pumped fluid through the secondary flow paths due to the larger bearing and impeller seals' diametric clearances. The primary goal of the labyrinth seals is to minimize reverse flow and recirculation of the operating fluid in the stages. The significant clearance change in the seals causes an increase in each stage's leakage and consequently dropped the pressure rise across each stage which in turn affected the entire performance of the pump. Another reason the pressure rise in the pump decreased with erosion time, but is not as a significant as the wear in the impeller seals, is the erosion of the primary paths including the impeller and diffuser vanes and walls. The changes in shape and dimension will increase the probability of eddies occurring in the primary flow path causing the loss of energy in the system. Signs of wear caused by these eddies is found on the impeller and diffuser walls, vanes and vane leading and trailing edges

Another example of impinging wear occurs on the diffuser blades causing more wear on the blades' pressure side than on the suction side. The flow around the blades has higher velocities on the suction side than on the pressure side and this should have given more wear on the suction side than on the pressure side. Opposite to the expected fluid dynamics general expected results, the solid particles in the fluid do not always follow the fluid's trajectory. In the mixed flow ESP pump the abrasive particles gain momentum due to the centrifugal forces and once they exit the impeller the abrasives impinge the diffuser's pressure side of the blades explaining the higher rate of wear seen.

Erosion greatly affected the vibration patterns and rotational patterns of the pump components. The rotor orbits constantly grew in diameter from 0 to 117 hours of testing. It was measured using proximeter probes at different locations of the pump. This orbital diameter increase is another direct result of the wider bearing and seal clearances cause by erosion wear. Following the same pattern of wear, the orbit diameter varies by location in the pump. Orbits are smaller near the drive end and are largest at the farthest location from the pump's drive end. The erosion of the bearings exceeded that of the impeller seals by at least 50% at 117 hours. This implies the impellers are replacing the bearings in carrying the rotor loads.
The waterfall plots of the pump rotor (impellers and shaft) oscillatory motion at base condition had peaks at the synchronous speeds only. As time progressed new peaks started appearing after only 24 hours at 33% and 67% of the synchronous. Finally after 117 hours, the sub-synchronous peak

at 67% had a larger magnitude than the synchronous peak indicating that the pump rotor started resonating at its critical speed, 2500 RPM. (A rotor ring test was performed by hanging the assembled rotor in air and then impacted.) The system's vibration response as a whole changed with time in all locations of the pump. As the bearing and seal clearances increased due to wear the rotor lost stiffness and reached the point where the rotor vibration locked with the rotor's natural frequency at around 2500 RPM. There was no reverse precession due to friction. Although the whole system's first critical was never reached in the 117 hours of testing, the rotor vibration plots, orbits and wear indicate that the rotor and its components have begun to resonate at their critical speeds. The mode of vibration is different in the synchronous and sub-synchronous vibrations. The sub-synchronous has a constant phase along the length of the rotor showing all elements are orbiting in unison, in a whirling motion. The synchronous motion has approximately one and a half cycles along the length of the shaft that was instrumented.

From the above discussion of the test results after 117 hours, it can be concluded that the most critical component of the ESP is the rotor. It includes the shaft, impellers, sleeve bearings, and sleeve spacers. The largest amount of wear was detected on the impeller seals and bearings. This affected the pump's overall performance. The rotor waterfall plots indicate that the rotor vibration has locked at the first critical speed of the rotor. This caused an increase in the rotor components rate of wear and the detection of damage to the components. It is recommended that the generic tungsten carbide bearings used in ESP pumps be replaced with bearings that are more tolerant to rubbing (resulting in thermal stress cracks) and modified in design to help flush sand from the bearing before severe gouging of the bearing surface occurs.

NOMENCLATURE

BEP = Best Efficiency Point
ESP = Electric Submersible Pump
PP = Proximeter Probe

REFERENCES

[1] Schlumberger, 2004, "Oilfield Review Summer 2004," pp. 4-66.

ACKNOWLEDGEMENTS

This project was sponsored by Shell under the supervision of Dr. Stuart Scott and Hector Casillas.